Journal of Alloys and Compounds 506 (2010) 249–252

Contents lists available at ScienceDirect

Journal of Alloys and Compounds

journal homepage: www.elsevier.com/locate/jallcom

Temperature dependence of morphology, structural and optical properties of ZnS nanostructures synthesized by wet chemical route

M. Navaneethan[a,c], J. Archana[a], K.D. Nisha[b], Y. Hayakawa[c], S. Ponnusamy[a,*], C. Muthamizhchelvan[a]

[a] Center for Materials Science and Nano Devices, Department of Physics, SRM University, Kattankulathur 603 203, Kancheepuram (D.t), Tamil Nadu, India
[b] Department of Physics, Asan Memorial College of Engineering and Technology, Chengalpattu 603105, Tamil Nadu, India
[c] Research Institute of Electronics, Shizuoka University, 3-5-1 Johoku, Naka-ku, Hamamatsu, Shizuoka 432-8011, Japan

ARTICLE INFO

Article history:
Received 24 March 2010
Received in revised form 23 June 2010
Accepted 1 July 2010
Available online 7 July 2010

Keywords:
Nanostructured materials
Optical materials
Semiconductors
Chemical synthesis
Luminescence

ABSTRACT

ZnS nanostructures have been synthesized by simple wet chemical route and annealed at two different temperatures of 50 °C and 180 °C. From the measurements of transmission electron microscopy and contact-mode atomic force microscopy, it is found that annealed temperature changes the morphology from nanoparticles to nanorods. The optical properties of the synthesized ZnS nanomaterial have been characterized by UV–visible absorption spectroscopy and photoluminescence spectroscopy. The structural and elemental analyses were carried out by powder X-ray diffraction pattern and energy dispersive X-ray absorption spectroscopy, respectively. Absorption edge of the nanoparticles (295 nm) and nanorods (326 nm) was shifted towards shorter wavelength compared to bulk ZnS (337 nm) due to the quantum confinement effect.

1. Introduction

In the past decade, semiconducting nanoparticles have received a considerable attention because of their excellent size dependent electrical and optical properties suitable for applications in optoelectronic devices [1,2]. Since the optical band gap of these semiconductors can be tuned by varying the size of the particles, these tuned optical properties of the materials have potential applications in the field of solar cell [3], light emitting diode [4], telecommunications [5], etc. Among the semiconducting particles, II–VI binary semiconductors are widely used in technological application. In particular, ZnS has a wide band gap of 3.68 eV, it is widely used in cathode ray tubes and field emission display [6], electroluminescent devices [7] and photodiodes [8]. Several methods have been adopted for the synthesis of nanoparticles, such as wet chemical method [9], microwave irradiation [10], micro emulsion [11], chemical vapor deposition [12], etc. ZnS can be synthesized by different routes, such as chemical route, microwave irradiation, etc.

In the present work, ZnS nanostructures were synthesized by wet chemical route without non toxic precursors annealed at two different temperatures. Surface morphology and structural property have been measured by atomic force microscopy (AFM), transmission electron microscopy (TEM) and X-ray diffraction (XRD). The optical properties of the synthesized materials were investigated by ultra violet (UV) spectrophotometer and photoluminescence (PL) spectrophotometer. The elemental analysis has been performed by energy dispersive X-ray spectroscopy (EDAX).

2. Experimental

All chemicals used were of analytical grade without further purification. ZnS nanoparticles were synthesized using zinc acetate and thioacetamide as source materials. 0.2 M Zinc acetate and 0.2 M thioacetamide were dissolved in 50 ml of ethanol and stirred at a constant rate for 8 h. This resulted in a milky white solution, indicating the formation of ZnS. Subsequently, the resulting milky white solid products were centrifuged and washed using ethanol. Finally, a part of the product (sample A) was dried at temperature of 50 °C for 10 h and remaining part (sample B) was dried at 180 °C in hot air oven for 10 h.

AFM studies were carried out with Pico Scale SPM (Molecular Imaging, USA). TEM images were taken with JEM 3010(JEOL) TEM with an accelerating voltage of 200 keV. X-ray diffraction (XRD) pattern was recorded using X'perPRO (PANalytical) advanced X-ray diffractometer with CuKα_1 radiation (λ = 1.5406 Å), with 2θ ranging between 20° and 80° at a scanning rate of 0.5°/s. Absorption spectrum was measured using PerkinElmer lambda 5 UV–visible spectrophotometer. PL spectrum was obtained using Flurolog-3 spectrophotometer (Jobin Yvon) in the range 200–900 nm. EDAX analysis was performed by Hitachi S 3400 SEM working at 25 kV accelerating voltage. Ethanol was used as a medium to prepare the sample for UV, PL, AFM and TEM studies.

3. Results and discussion

Fig. 1(a) shows the AFM image of sample A annealed at temperature of 50 °C and it reveals the formation of nanoparticles. In this image, all the particles exhibited uniform size and spherical

* Corresponding author. Tel.: +91 44 27452818; fax: +91 44 27456255.
E-mail address: suruponnus@gmail.com (S. Ponnusamy).

0925-8388/$ – see front matter © 2010 Elsevier B.V. All rights reserved.
doi:10.1016/j.jallcom.2010.07.002

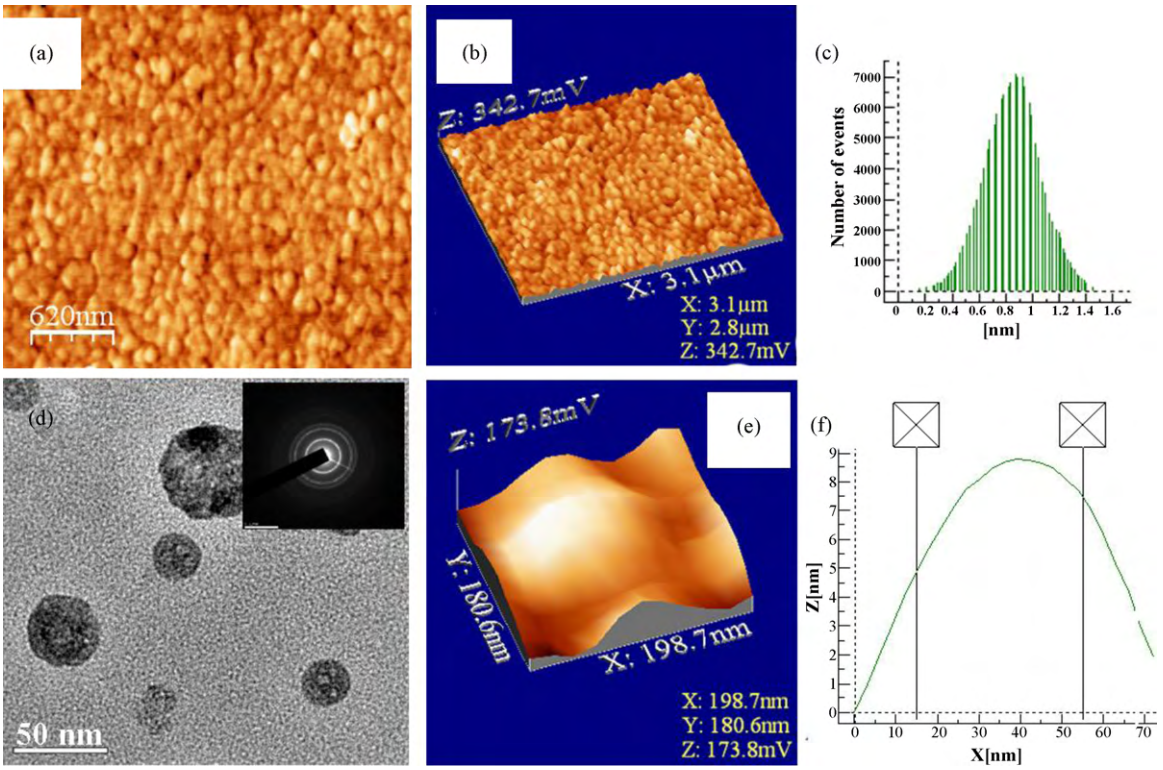

Fig. 1. (a) AFM image of sample A (ZnS nanoparticles) (b) 3D view of ZnS nanoparticles (c) Roughness analysis (d) TEM micrograph of ZnS nanoparticle (inset: SAED pattern) (e) 3D view of an individual ZnS nanoparticle (f) Size profile of an individual ZnS nanoparticle.

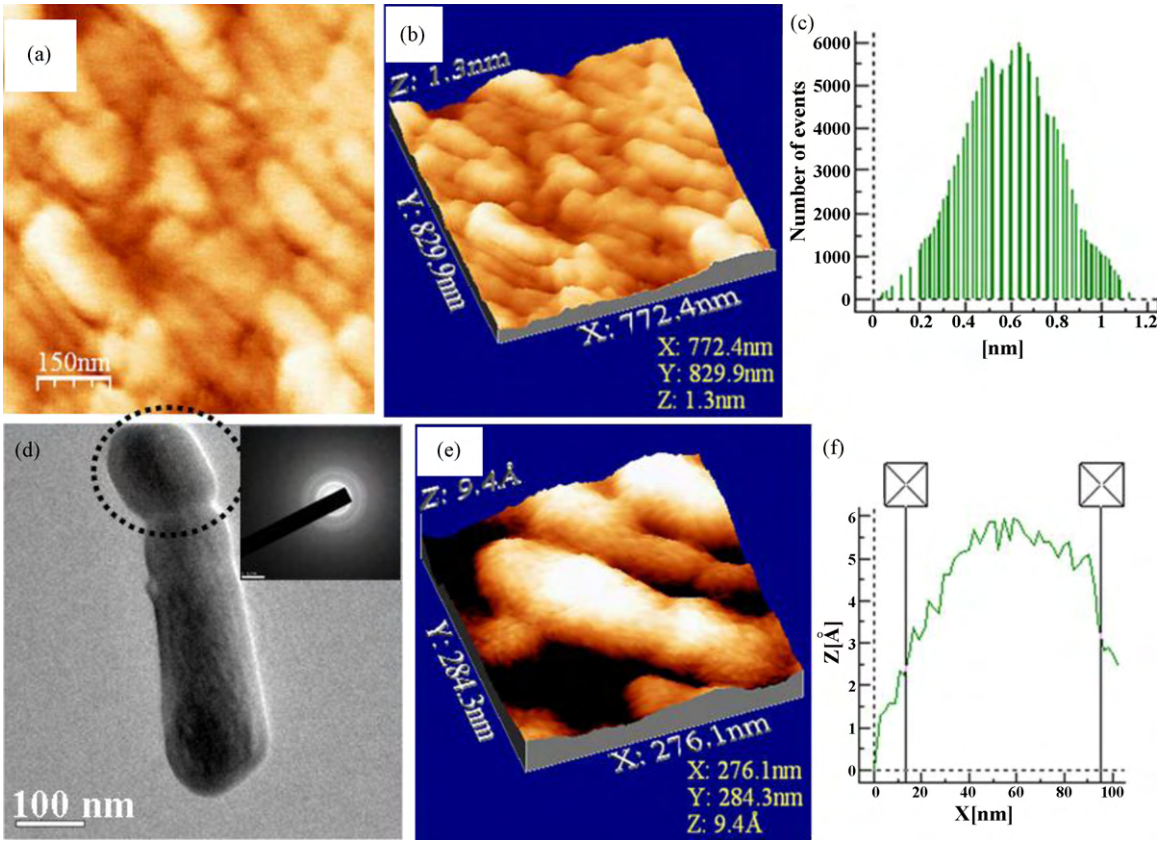

Fig. 2. (a) AFM image of sample B (ZnS nanorods) (b) 3D view of ZnS nanorods (c) Roughness analysis (d) TEM micrograph of an individual ZnS nanorod (inset: SAED pattern) (e) 3D view of an individual ZnS nanorod (f) Width profile of an individual ZnS nanorod.

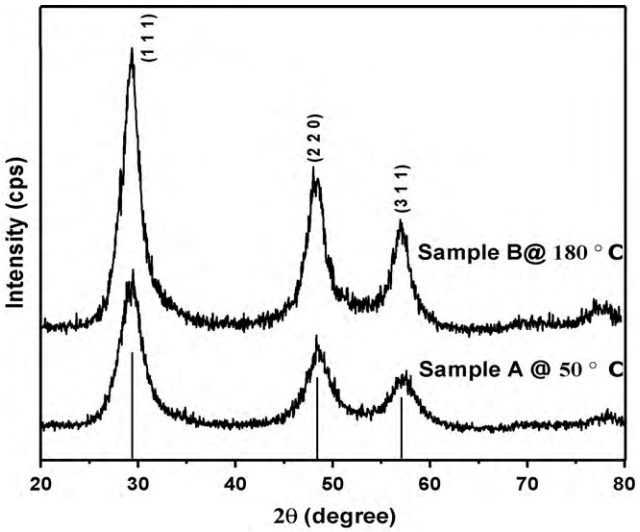

Fig. 3. XRD pattern of ZnS nanoparticles and ZnS nanorods.

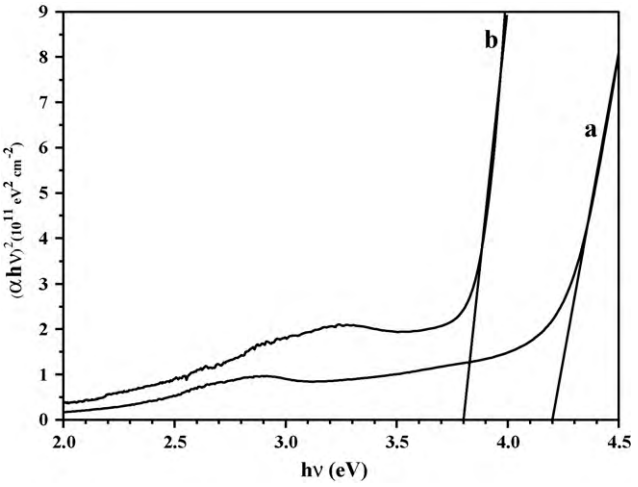

Fig. 5. Bandgap plot $h\nu$ vs $(\alpha h\nu)^2$ of ZnS nanoparticles and ZnS nanorods.

in shape without agglomeration. All the particles were easily distinguishable. Sizes of the synthesized ZnS nanoparticles (sample A) were in the order of 35–55 nm with uniform distribution. The 3D view of the ZnS nanoparticles is shown in Fig. 1(b); it revealed that the growth direction of all particles was same. Fig. 1(c) shows the roughness analysis of the synthesized ZnS nanoparticles, it was observed that the roughness of the particles was in uniform distribution of few nanometers. The height of the particles from the substrate was found to be 0.4–1.2 nm and maximum number of counts is around 0.9 nm. Fig. 1(d) shows the TEM micrograph of ZnS nanoparticles, it shows that all the particles were free from agglomeration with the size of 30–50 nm. This is well consistent with the AFM results. Ring patterns were observed in the SAED pattern of ZnS nanoparticles (inset of Fig. 1(d)), which clearly indicated the formation of polycrystalline nature of ZnS nanoparticles. 3D view of an individual ZnS nanoparticle is shown in Fig. 1(e). It is clearly seen that the size of an individual nanoparticle was 40 nm as shown in Fig. 1(f).

Fig. 2(a) shows the AFM image of sample B. It is clearly indicated that the formation of rod like structures. Also the shape and size of the nanorods were easily distinguishable. In order to know the shape evolution in three directions of the ZnS nanorods (sample B), the typical 3D projection view of the ZnS nanorods is depicted in Fig. 2(b). The formation of nanorods is as follows: Due to the thermal heating, the self-aggregation has taken place between the nanoparticles and it leads to the formation of nanorods [13]. Further the Ostwald ripening may cause the random oriented self-aggregation in the nanoparticles because the free energy is reduced by decreasing the number of small nanoparticles [14]. The similar results were observed by Ghosh et al. [15]. The roughness analysis of the ZnS nanorods is shown in Fig. 2(c). The roughness of the nanorods was around 0.4–0.8 nm. The maximum numbers of the rods were in the height of 0.6 nm. It shows that the roughness of the nanorods was less than that of nanoparticles (sample A) due to their surface changes from the nanoparticles to nanorods. Fig. 2(d) shows TEM micrograph of an individual ZnS nanorods. Diameter of the nanorod is around 150 nm. The formation of the self-aggregated particles was clearly seen in the marked area. Further, this is well consistent with AFM results. SAED pattern of ZnS nanorods (inset of Fig. 2(d)) clearly indicates the formation of polycrystalline ZnS nanorods. Fig. 2(e) shows the 3D projection of an individual ZnS nanorods. The domains of the nanoparticles were clearly seen in this image. Also the height of the ZnS nanorod in the *Z*-direction was well consistent with the roughness analysis of the ZnS nanorods shown in Fig. 2(c). The width profile of an individual ZnS nanorod is shown in Fig. 2(f) and its width is found to be 80 nm.

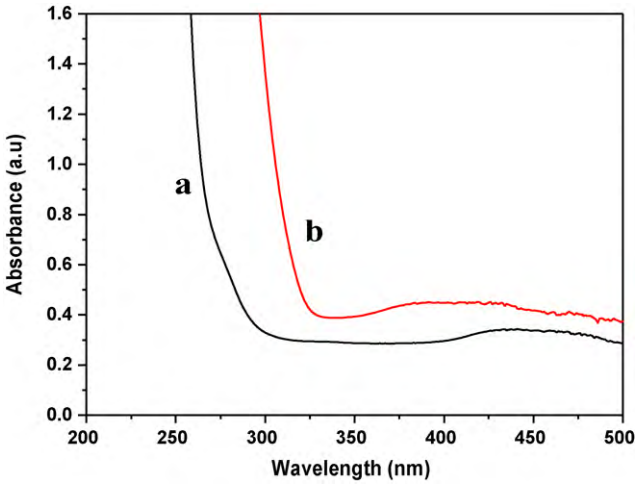

Fig. 4. UV–visible absorption spectra of ZnS nanoparticles and ZnS nanorods.

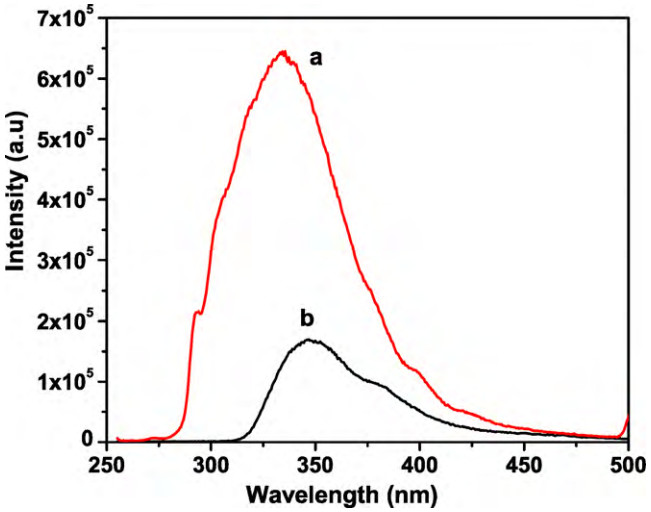

Fig. 6. Photoluminescence spectra of ZnS nanoparticles and ZnS nanorods.

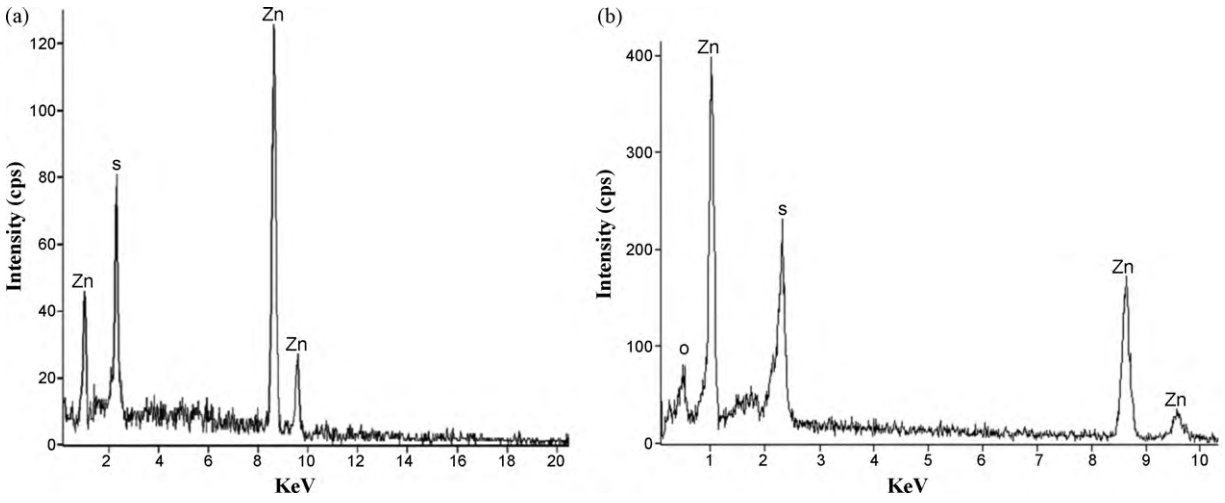

Fig. 7. EDAX analysis of ZnS nanoparticles and ZnS nanorods.

XRD pattern of ZnS nanoparticles and ZnS nanorods are shown in Fig. 3. Both the samples exhibited similar peaks corresponding to (1 1 1), (2 2 0) and (3 1 1) planes with cubic phase of ZnS. XRD pattern of the synthesized ZnS nanoparticles was well matched with the standard JCPDS data (Card No. 05- 0566). Broadening of the peaks indicates the formation of nanoparticles. The peak broadening of ZnS nanoparticles was higher than that of ZnS nanorods. It shows the particle size increased during heating. These results were consistent with the AFM results of the samples.

UV–visible spectra of ZnS nanoparticles and ZnS nanorods are shown in Fig. 4. Absorption edge of ZnS nanoparticles is 295 nm and that of ZnS nanorods is 326 nm. It indicates that absorption edges of ZnS nanoparticles and ZnS nanorods were shifted towards "blue" compared to ZnS bulk (337 nm). The bandgap plots of ZnS nanoparticles and ZnS nanorods are shown in Fig. 5. The bandgap of ZnS nanoparticles was 4.2 eV and the bandgap of ZnS nanorods was 3.8 eV. Bandgap of the ZnS nanorods was shifted towards the red side compared to that of ZnS nanoparticles due to aggregation of the particles. It indicates that the size of the particles was associated with the bandgap and the size increase on annealing was confirmed through the AFM and TEM studies. Photoluminescence spectra of ZnS nanoparticles and ZnS nanorods are shown in Fig. 6. Photoluminescence emission peaks were obtained for the excitation wavelength of 250 nm. The emission peak was observed at 333 nm for ZnS nanoparticles and 345 nm for ZnS nanorods. The significant blue shift of nanoparticles was observed due to the quantum confinement. The difference between the absorbance and emission peaks was around 38 nm (nanoparticles) and 19 nm (nanorods). This is due to the trap state emission of the smaller size particles. Also the defects could be attributed to the vacancy of sulfur in the nanoparticles [16]. The intensity of the emission peak of nanorods was comparatively less than that of nanoparticles, and the peak was shifted towards the longer wavelength. The intensity of the emission peak was strongly affected by the temperature. The luminescence quenching of the sample B was due to the self-aggregation of the particles. Typical EDAX analysis of sample A and sample B are shown in Fig. 7(a) and (b), respectively. The strong peaks of Zn and S were clearly seen in the spectrum. No other peaks related to impurities were observed in the sample A. But, in the case of sample B, a low intensity peak related to oxygen atom was observed. It may be due to oxidation of surface of the sample during the annealing process in hot air oven. However, no other peaks related to the formation of ZnO were observed in XRD pattern of sample B. Further it confirms that the synthesized material was composed of ZnS.

4. Conclusion

ZnS nanoparticles and nanorods have been synthesized by wet chemical route. Higher annealing temperature influenced the change in morphology due to aggregation of the nanoparticles. The temperature dependent optical properties were investigated. Absorption edge of nanoparticles (295 nm) and nanorods (326 nm) were shifted towards shorter wavelength compared to bulk ZnS (337 nm) due to the quantum confinement effect. ZnS nanoparticles exhibit high photoluminescence intensity than that of ZnS nanorods annealed at 180 °C.

Acknowledgement

One of the authors M. Navaneethan is thankful to the SRM UNIVERSITY for providing the research fellowship.

References

[1] J.M. Bruchez, M. Moronne, P. Gin, S. Weiss, A.P. Alivisatos, Science 281 (1998) 2013–2016.
[2] L.E. Brus, J. Chem. Phys. 80 (1984) 4403–4409.
[3] W.U. Huynh, J.J. Dittmer, N. Teclemarian, D.J. Milliron, A.P. Alivisatos, K.W. Barnham, J. Phys. Rev. B 67 (2003) 115326–115337.
[4] V.L. Colvin, M.C. Schlamp, A.P. Alivisatos, Nature (1994) 354–357.
[5] D.L. Klein, R. Roth, A.K.L. Lim, A.P. Alivisatos, P.L. McEuen, Nature 389 (1997) 699–701.
[6] R. Mach, G.O. Muller, J. Cryst. Growth 86 (1990) 866–872.
[7] R. Vacassy, S.M. Scholz, J. Dutta, H. Hofmann, C.J.G. Plummer, G. Carrot, J. Hilborn, M. Akine, Mater. Res. Soc. Symp. Proc. 501 (1998) 369.
[8] T. Yamamoto, S. Kishimoto, S. Iida, Physica B 308 (2001) 916–919.
[9] A.A. Khosic, M. Kundu, L. Jatwa, S.K. Deshpande, U.A. Bhagwat, M. Sastry, S.K. Kulkarni, Appl. Phys. Lett. 67 (1995) 2702–2704.
[10] Eugenio Caponetti, Delia Chillura Martino, Maurizio Leone, Lucia Pedone, Maria Luisa Saladino, Valeria Vetri, J. Colloid Int. Sci. 304 (2006) 413–418.
[11] Jianling Zhang, Buxing Han, Juncheng Liu, Xiaogang Zhang, Guanying Yang, Huaizhou Zhao, J. Supercrit. Fluids 30 (2004) 89–95.
[12] Tianyou Zhai, Zhanjun Gu, Ying Ma, Wensheng Yang, Liyun Zhao, Jiannian Yao, Mater. Chem. Phys. 100 (2006) 281–284.
[13] W.Z. Wang, C.K. Xu, G.H. Wang, K.L. Liu, C.L. Zheng, Adv. Mater. 14 (2002) 837–840.
[14] Chun Lan, Kunquan Hong, Wenzhong Wang, Kunquan Hong, Guanghou Wang, Solid State Commun. 125 (2003) 455–488.
[15] P.K. Ghosh, U.N. Maiti, S. Jana, K.K. Chattopadhyay, Appl. Surf. Sci. 253 (2006) 1544–1550.
[16] K. Manzoor, V. Aditya, S.R. Vadera, N. Kumar, T.R.N. Kutty, J. Phys. Chem. Solids 66 (2005) 1164–1170.